Proposal and Evaluation of Subordinate Standard Solar Irradiance Spectra with a Focus on Air Mass Effects

Stefan Wilbert[1], Wilko Jessen[1], Chris Gueymard[2], Jesús Polo[3], Zeqiang Bian[4], Anton Driesse[5], Aron Habte[6], Aitor Marzo[7], Peter Armstrong[8], Frank Vignola[9], Lourdes Ramírez[3]

[1]DLR, German Aerospace Center, Ctra de Senes s/n km4 04200 Tabernas, Spain. Stefan.Wilbert@dlr.de

[2]Solar Consulting Services, P.O. Box 392 Colebrook, NH 03576, USA

[3]CIEMAT, Avda Complutense, 40 Madrid 28040 Spain

[4]China Meteorological Administration No.46 Zhonguancun Nandajie Bejing 100081China

[5]Photovoltaic Performance Labs, Emmy-Noether-Str. 2 Freiburg 79110 Germany

[6]NREL 15013 Denver West Parkway Golden 80401 USA CO

[7]Centro de Desarrollo Energético Antofagasta (CDEA), University of Antofagasta Av. Angamos, 601 Antofagasta 1270300 Chile

[8]Masdar Institute, Khalifa University of Science & Technology, PO Box 54224 Abu Dhabi, United Arab Emirates

[9]Univ. of Oregon, 1274 Univ. of Oregon Eugene OR 97403-1274, USA

Abstract

This paper introduces a concept for global tilted irradiance (GTI) subordinate standard spectra to supplement the current standard spectra used in solar photovoltaic applications, as defined in ASTM G173 and IEC60904. The proposed subordinate standard spectra correspond to atmospheric conditions and tilt angles that depart significantly from the main standard spectrum, and can be used to more accurately represent various local conditions. For the definition of subordinate standard spectra cases with an elevation of 1.5 km above sea level the question arises whether the air mass should be calculated including a pressure correction or not. This study focuses on the impact of air mass used in standard spectra, and uses data from 29 locations to examine which air mass is most appropriate for GTI and direct normal irradiance (DNI) spectra. Overall, it is found that the pressure corrected air mass of 1.5 is most appropriate for DNI spectra. For GTI a non-pressure-corrected air mass of 1.5 was found to be more appropriate. The suitability of this selection for a given site is best for mid latitudes (~35°) and elevations below 1 km. It also depends on the vertical distributions of aerosols and water vapor.

Keywords: solar spectra, efficiency rating, spectral response, standardization, air mass

1. Introduction

Standard solar irradiance spectra are required to compare and specify key parameters of solar technologies, such as the efficiency of photovoltaic (PV) cells. In particular, the recent IEC standard 60904-3 prescribes a Direct Normal Irradiance (DNI) spectrum and a Global Tilted Irradiance (GTI) spectrum for a 37° tilted sun-facing surface, both defined for a clear-sky condition with air mass 1.5 (AM1.5) and low aerosol content. The IEC spectra are identical to the ASTM G173 spectra when scaled by a factor of 0.99708. These reference spectra are widely used for rating purposes when different products, such as PV cells, have to be compared under Standard Test Conditions (STC), as discussed by, e.g., Gueymard et al. (2002). To maintain comparability of results, it is important that a single standard spectrum for either GTI or DNI be used for the purpose. The present authors are also working towards replacing the current (but outdated) ISO 9845 spectra by the IEC spectra just mentioned within the ongoing update of the ISO standard.

The unique importance of the IEC (or ASTM) spectra is not at all called into question in this work. However, these reference spectra may differ strongly from realistic average spectra at sites with different atmospheric

doi:10.18086/swc.2017.21.06 Available at http://proceedings.ises.org

conditions or for tilt angles that are different from 37°. For such cases, it is useful to compare products using both the standard spectra and additional subordinate reference spectra that correspond better to specific local atmospheric conditions and sun-receiver geometries than the standard spectra. In particular, it should be noted that the current standards only represent sea-level conditions. High-elevation sites tend to have higher solar resource, which attracts many solar energy projects. In the case of small installations, for instance, such a rough comparison can be helpful as a simple product pre-selection tool when sophisticated performance evaluation is not feasible. For larger installations requiring more sophisticated evaluations, this kind of comparison may reduce the effort by decreasing the number of initial product candidates.

The impacts of the incident spectrum on the performance of different PV cell technologies have been studied using both measured and modeled solar spectra (Fernandez et al., 2014; Nofuentes et al., 2017; Dirnberger et al., 2015; Polo et al., 2017). These publications show the importance of atmospheric conditions on the magnitude and shape of incident spectra and underline the need for specific methods to evaluate spectral effects in yield analyses. One way to improve the state-of-the-art in PV modeling is to provide subordinate standard spectra that cover situations beyond what the ASTM G173/IEC 60904-3 standards are meant to address.

Section 2 below briefly presents suggestions for subordinate standard spectra corresponding to eight sets of atmospheric conditions and a range of tilt angles that are currently considered within the ISO working group. High-elevation locations (1.5 km above sea level) are included as well. Section 3 discusses the proper definition of air mass in the case of elevated sites. To this end, the cumulative annual direct normal and global tilted irradiations are analyzed as a function of air mass, based on irradiance measurements at 29 sites. Furthermore, the average solar spectra for two elevated sites are analyzed to establish which definition of air mass to use. Finally, a conclusion and an outlook are presented.

2. Proposed subordinate standard spectra

Subordinate GTI spectra are proposed for nine atmospheric conditions defined in terms of aerosol optical depth at 500 nm (AOD500), precipitable water vapor (PW), and elevation, as given in Table 1. The suggested tilt angles are from 0° to 90° in increments of 5°. To limit the number of subordinate spectra other parameters such as the azimuth orientation of the surface are not varied. Exemplary spectra for a tilt angle of 20° are shown in Fig. 1. As in the existing standards, AM1.5 is used. Why this specific air-mass value was selected originally is discussed elsewhere (Ross and Gonzalez, 1980; Gueymard et al., 2002). To be clear, the air mass indicates the *relative* (non-pressure corrected) air mass value M_{npc}. A discussion on various definitions of air mass appears in the next section. Additionally, DNI spectra for the same atmospheric conditions are also investigated, but are not shown graphically since they are not recommended as subordinate standard spectra. However, the air mass selection for DNI spectra is specifically discussed in what follows.

Tab. 1: Suggested conditions for the GTI subordinate standard spectra, below those used in (IEC, 2016). All cases use the aerosol type "rural" and the albedo "light sandy soil" except for DustyMedHum, for which "Desert_Max" and "dune sand" are used. The abbreviations used to describe the atmosphere are defined in (Gueymard, 2005).

Short name	Description	Elev. (km)	AOD@ 500nm	PW (cm)	Representative Atmosphere
IEC 60904	Reference (IEC 60904-3)	0	0.084	1.416	USSA
SemClmedHum	Semi-clean, medium humidity, sea level	0	0.27	1.416	USSA
SemClHum	Semi-clean, humid, sea level	0	0.27	4.115	TRL
HazMedHum	Hazy, medium humidity, sea level	0	0.54	1.416	USSA
DustyMedHum	Dusty, medium humidity, sea level	0	0.54	1.416	STS
HazHum	Hazy, humid, sea level	0	0.54	4.115	TRL
ClDryHi	Clean, dry, high elevation	1.5	0.084	0.708	MLW
SemClDryHi	Semi-clean, dry, high elevation	1.5	0.27	0.708	MLW
HazDryHi	Hazy, dry, high elevation	1.5	0.54	0.708	STW

Some aspects of the existing IEC/G173 standard spectra that can be considered outdated are modified here for creation of the proposed subordinate spectra. The first of these aspects is related to circumsolar radiation. DNI is defined in terms of the viewing geometry of a pyrheliometer following the WMO recommendations for a slope angle of 1° and an opening angle of 2.5° (WMO, 2014). In IEC/G173 this opening angle was slightly larger (2.9°).Second, the newer SMARTS version 2.9.5 (Gueymard, 2001, 2005) is used here to construct the proposed subordinate spectra as opposed to v2.9.2 that was used for the current standards. Third, the solar constant of 1361.2 W/m² (Gueymard, 2012) replaces the outdated historical value of 1367 W/m² (see justification in Kopp and Lean, 2011). The extraterrestrial spectrum (ETR) selected within SMARTS is still "Gueymard, synthetic" (as was used in the current standards) but multiplied by 1361.2/1367. Spectral changes resulting from all of the above relative to G173 are minor, as shown in Fig. 2.

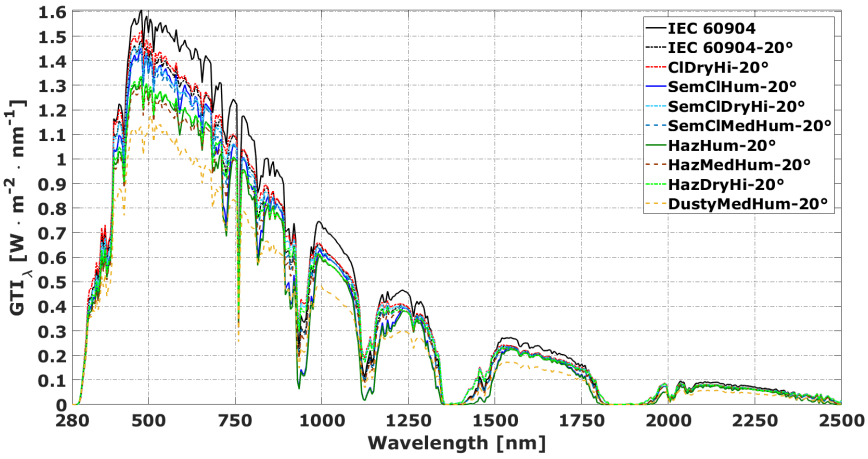

Fig. 1: Proposed subordinate standard spectra for GTI on a surface tilted 20° toward the equator.

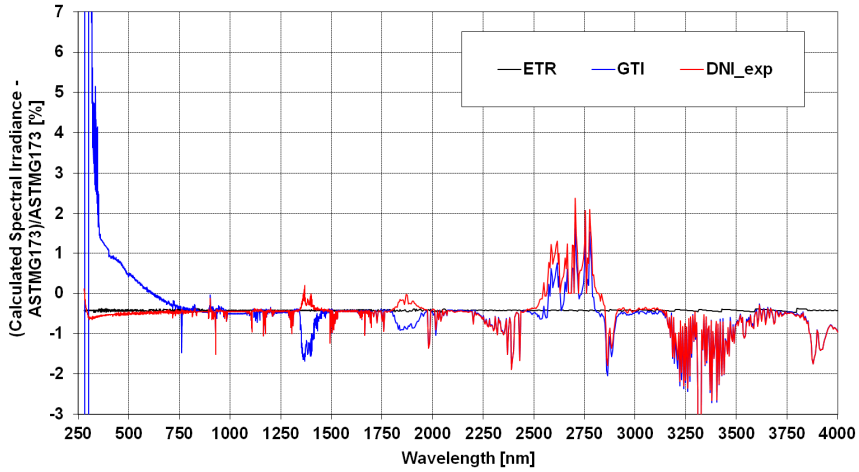

Fig. 2: Effect of changed circumsolar radiation settings, solar constant and SMARTS version, relative to the corresponding DNI and GTI spectra promulgated in G173 (red and blue line). The change of the extraterrestrial spectrum is shown in black.

The responsivity of a PV cell relative to an incident broadband solar irradiance, is obtained by multiplying its spectral responsivity, R_λ, with the solar irradiance spectrum, E_λ, according to

$$R_S = \frac{\sum_{j=1}^{N} R_\lambda(\lambda_j) \cdot E_\lambda(\lambda_j) \cdot \Delta\lambda_j}{\sum_{j=1}^{N} E_\lambda(\lambda_j) \cdot \Delta\lambda_j} \qquad \text{(eq. 1)}$$

where λ_j is the jth wavelength in the series 1–N. The relative deviation between the R_S value for a test spectrum and that for a reference spectrum is the spectral mismatch δ_{RS}. It can refer to a spectral gain or a spectral loss.

In a related study (Jessen et al., 2018), the proposed subordinate GTI spectra are compared to each other in terms of irradiance and PV device efficiency, using the spectral responsivities of exemplary solar cells from Winter et al. (2009), with or without concentration. The results show that the proposed subordinate spectra generate significant spectral mismatches compared to the IEC spectra (up to 6.5 %, for PV cells at a 37° tilt). Such mismatches indicate potential accuracy improvements that become possible by applying the subordinate standard spectra rather than the IEC spectra for a quick estimation of the *average* device efficiency.

To apply the subordinate standard spectra, manufacturers of solar devices could include PV module efficiencies for the different subordinate spectra in their data sheets. Alternatively, the spectral mismatches between using the IEC/G173 spectra and the subordinate spectra could be stated. A potential customer could then identify the potential change in efficiency based on a site's average AOD500, PW, elevation, and tilt angle. Consideration of all combinations of the aforementioned parameters with a tilt angle step of 5° would result in 171 efficiency values for PV panels, which could be conveniently presented by plotting the efficiency as a function of tilt angle. In case the manufacturer provides the spectral response rather than these values, a potential customer could independently calculate the specific mismatch between results based on either the IEC/G173 spectrum or the relevant subordinate spectrum, and thus estimate the changes in efficiency. Another advantage of these subordinate spectra is that they can assist in characterizing the durability of PV, CPV and CSP materials ex-

posed to natural weathering at a site.

A simple procedure to select subordinate standard spectra based on a site's average AOD500, PW, elevation and tilt angle was tested by Jessen, et al, (2018) at five exemplary sites [Tamanrasset, Sede Boker and Boulder (Baseline Surface Radiation Network, BSRN, König-Langlo et al., 2013), Plataforma Solar de Almería (PSA, Wilbert et al., 2013, Pozo et al., 2011), and Masdar (Kalapatapu et al., 2012)]. Two of these test sites, Tamanrasset and Boulder, are also used in this study. In Fig. 3, the average AOD500 and PW values for the annual data sets that were evaluated at these sites are shown next to the available AOD500 and PW values from the nine suggested atmospheric conditions. At all five test sites, complete time series of spectra (including both clear and cloudy periods) are determined using a combination of the SMARTS model and SEDES2 cloud modifiers (Nann and Riordan, 1991), with inputs based on site-specific sun-photometer and shortwave irradiance measurements. From all these all-sky spectra a site-specific annual-average spectrum is derived as a reference for the applicability test. In these reference spectra the impact of clouds is introduced through the use of SEDES2 in order to obtain realistic average spectra including the effect of clouds. For the subordinate standard spectra we propose only clear-sky spectra because clear sky conditions contribute stronger to the yield than most cloudy conditions and for simplicity. The resulting site-specific spectral mismatch values for the subordinate standard spectra and the IEC spectrum with respect to the site's average spectrum were derived. The subordinate spectrum with the most similar conditions to the site average results in a much lower spectral mismatch than the G173 spectrum (Jessen et al., 2018). Therefore, the proposed GTI spectra are applicable to the five test cases. Tests with other sites, for example with higher PW are of interest. For CSP and CPV applications, however, the suggested atmospheric conditions are found insufficient, due to the strong effects of AOD and Ångström exponent on DNI (Jessen et al., 2018). Hence, it is not intuitively possible to pick the most appropriate DNI spectrum from the subordinate spectra. Many more sets of atmospheric conditions would be required to allow the intuitive selection of a representative spectrum for the five test sites, let alone any other site. Hence, only GTI spectra with tilt variation are suggested for implementation in future standards.

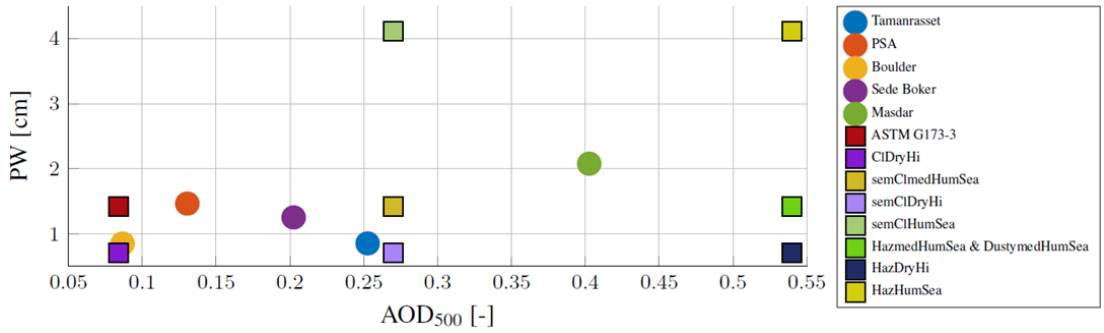

Fig. 3: AOD500 and PW for subordinate standard spectra (squares) and their averages for the sites (circles) that are used to test the intuitive selection of an appropriate reference spectrum. Matching colors mark the specific reference spectrum that would be selected based on a site's AOD500, PW and elevation.

3. Selection of air mass for the subordinate standard spectra

Besides the three AOD500 and three PW categories, an additional site elevation category of 1.5 km is suggested in Table 1 to extend the applicability of subordinate standard spectra. Introduction of high-elevation subordinate spectra raise the question of whether a pressure-corrected (absolute) or non-corrected (relative) definition of air mass is preferable. Note first that "air mass" itself is an ambiguous term. The *relative air mass* is a quantity that would be better called "optical mass for air molecules", since it corresponds to the geometric path length of the sun rays traversing the atmosphere relative to the vertical path length, and is a function only of the sun's zenith angle, *Z*. This quantity takes atmospheric refraction and Earth sphericity into account, and is thus more appropriate than the conventional 1/cos*Z* factor used in the plane-parallel approximation that is typical in radiative transfer. Optical masses for aerosols, water vapor or ozone differ from the optical air mass because their concentrations have different vertical profiles. SMARTS, for instance, uses 15 different optical masses, corresponding to as many atmospheric species (or groups of species), because they have different vertical profiles. In contrast, the *absolute air mass* is pressure-corrected to reflect the actual slant "optical mass of air molecules" at higher elevations. At the top of atmosphere, this absolute mass becomes 0, and is conventionally noted AM0. The optical depth due to Rayleigh scattering by air molecules decreases with elevation as a direct function of pressure, whereas optical depths of aerosols and water vapor have a different dependence on pressure, which is moreover highly variable over space and time. All this makes the use of air mass and pressure suscep-

tible to misinterpretation and confusion.

The choice of air mass has a direct impact on the resulting spectrum and needs to be considered carefully. If a high-elevation subordinate standard DNI spectra had to be defined with a pressure-corrected (PC) air mass, M_{pc}, of 1.5, the SMARTS input value for the *air mass* would need to be adjusted accordingly, since the SMARTS input must be a non-pressure corrected (NPC) value. The needed air mass input value for M_{pc} = 1.5 is M_{npc} ≈1.8, considering the ratio between the ambient pressure at 1500 m elevation (≈840 hPa) and 1013.25 hPa. The choice of input value leads to noticeably different solar zenith angles of 48.236° (for M_{npc} = 1.5) and 56.267° (for M_{npc} = 1.8). SMARTS does not actually consider any pressure correction for its optical masses. Instead, the optical depths related to Rayleigh scattering and uniformly-mixed gases are scaled by the pressure ratio. All other optical depths, including those for aerosols and water vapor, are independent from site pressure, because they are defined as column quantities between the surface (at any elevation) and the top of atmosphere. Hence, site elevation and pressure are already accounted for in the inputs for PW and AOD. Changing the relative air mass M_{npc} from 1.5 to 1.8, the pressure from 1013.25 hPa to 840 hPa, and the input elevation from 0 to 1500 m, while maintaining the same AOD input value, results in a noticeable change in the DNI spectrum, so this distinction is important.

In what follows, the air mass effect is investigated by two methods. First, the cumulative relative fraction of annual irradiation is calculated as a function of air mass to determine a characteristic air mass. Based on this, specific air mass values are recommended for the determination of DNI and GTI spectra. Then, for further analysis, the spectral mismatch is evaluated for a number of spectra derived with different air mass options.

3.1 Cumulative relative fraction of annual irradiation as a function of air mass

An appropriate air mass needs to be selected for each subordinate standard spectrum. To that effect, the distribution of annual irradiation over many sites is analyzed as a function of air mass. In the late 1970s, the NASA-recommended terrestrial PV measurement procedures already stipulated an air mass value of 1.5 for reference measurements. This AM1.5 "optimal" value was confirmed in interrelated studies (Gonzalez and Ross, 1980; Ross, 1980; Ross and Gonzalez, 1980) as most representative for performance evaluation of PV concentrators using DNI, but not for fixed-tilt flat-plate PV, based on conditions pertaining only to the continental United States. This was later confirmed by Emery et al. (2002) for DNI, still under U.S. conditions only. These results provide an argument for working with a pressure-corrected M_{pc} =1.5 for standard spectra in the case of DNI. The "pressure-corrected" adjective is emphasized. Assuming equivalence between a spectrum obtained for M_{npc} =1.5 at sea level and another one for M_{npc} =1.8 (or M_{pc} =1.5) at 1500 m would imply that the effects of AOD and PW on DNI decrease the same way as those of air molecules when elevation increases. Based on the discussion above, this might not be the general rule. Hence, further scrutiny will have to be given to this important topic, since it conditions the desirable generalization to any world location.

To determine the appropriate air mass for the subordinate standard spectra, the method used by Emery et al. (2002) is applied to a total of 29 sites from BSRN and enerMENA (Schüler et al., 2016) at latitudes from 30°S to 52°N, including five sites close to the equator (between 16°N and 16°S). Both DNI and GTI are investigated. Since GTI measurements are rare, the model from Skartveit and Olseth (1986) is used to estimate GTI on tilted surfaces oriented towards the equator and with tilt angles equal to each site's latitude. The model uses the measured DNI and GHI along with inputs including solar position, tilt angle, and surface albedo. The latter is set to 0.3 for all sites, which roughly corresponds to the albedo option "light sand" used in G173. Eighteen of the sites are below 750 m elevation while eleven are at higher elevations. With regard to the proposed subordinate standard spectra, a site above 750 m would be considered a high-elevation site.

Figure 4 presents the cumulative relative fraction of annual global tilted irradiation, H_{tilt}, in relation to two alternate definitions of air mass for sites below 750 m elevation. On the left side of Fig. 4, the Y-axis corresponds to the fraction of the annual global tilted irradiation that is received for pressure corrected air masses below the PC air mass given on the X-axis. The right hand side of Fig. 4 uses the NPC air mass. Interestingly, the intersection of some curves with the Y-axis corresponds to a cumulative H_{tilt} strictly positive (and up to 0.18) for the PC air mass. This is because PC air masses below 1 occur for elevated sites due to the pressure correction. On the other hand, some curves cross the X-axis at air masses greater than 1. These curves belong to sites far away from the equator (e.g., Regina, Canada) where the zenith angle is much larger than 0° even at solar noon in summer, so that the air mass never reaches values close to 1. Similarly to Fig. 4, Fig. 5 shows the cumulative H_{tilt} as a function of air mass for sites above 750 m. The difference between the two air-mass cases is much more pronounced here, since the pressure correction is more intense. As in Fig. 4, the PC curves are shifted

towards the left relative to the NPC curves.

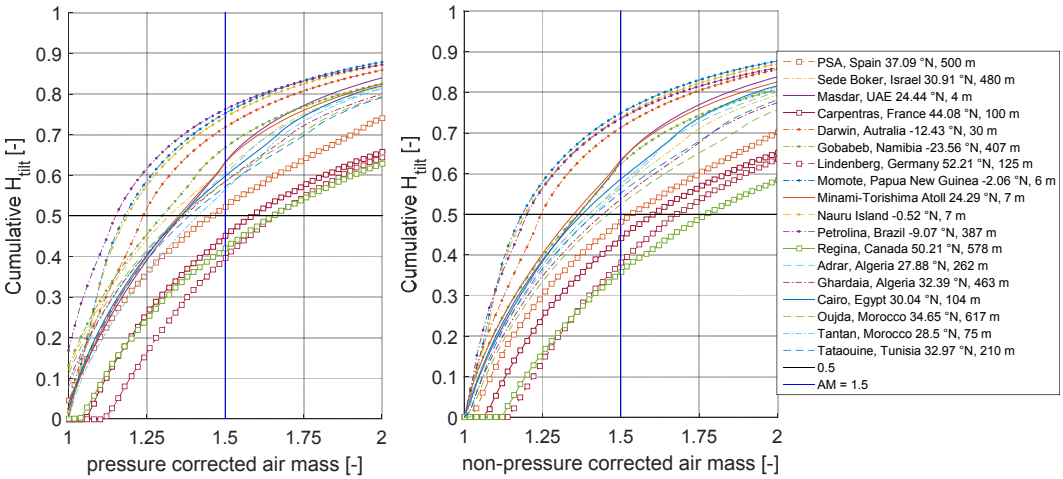

Fig. 4: Cumulative H_{tilt} over the air mass for sites below 750 m above mean sea level. Left: with pressure correction, right: without pressure correction. Sites less than 16° from the equator are marked with dots; sites at latitudes above 37° by squares.

To evaluate the effects of pressure correction and latitude in more detail, the results above are analyzed in terms of the threshold air mass, M_{half}, below which half of a site's total irradiation is received. M_{half} is indicated in Figs. 4 and 5 as the intersection of a site's curve and the horizontal line corresponding to a value of 0.5 on the Y-axis. Four different M_{half} values are derived for each site using PC and NPC air mass for GTI and using PC and NPC air mass for DNI. All M_{half} values for GTI are shown in Fig. 6 as a function of elevation (X-axis) and latitude (color bar). For both definitions of air mass, strong scatter is obvious. It is clear that an air mass value of 1.5 (or of any other fixed value) cannot accurately represent M_{half} at all investigated sites, irrespective of pressure correction. This shows a serious limitation of the approach considered in earlier studies (e.g., Emery et al., 2002), as well as the intrinsic limitation of reference spectra (standard or subordinate) that refer to a single air mass. However, for the simplification implied by the construction of the proposed subordinate spectra, this limitation must be acknowledged and accepted. Its effect, in terms of spectral mismatch, will be evaluated later after selecting single air mass values.

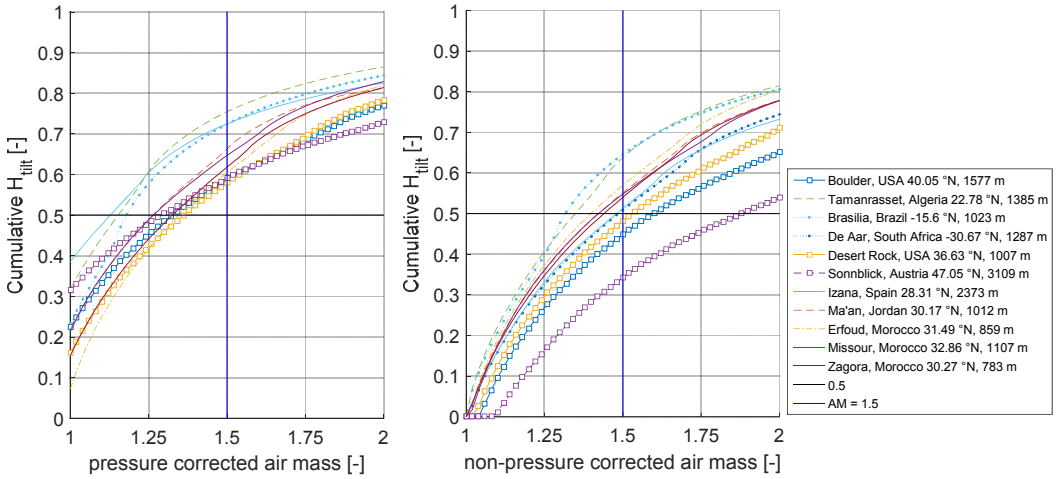

Fig. 5: Cumulative H_{tilt} as a function of the air mass for sites at elevations above 750 m. Left: with pressure correction, right: without pressure correction. Sites less than 16° from the equator are marked with dots; sites at latitudes above 37° by squares.

The spread of M_{half} values found for any small elevation range is related to latitude. Due to the higher solar elevation angles, proximity to the equator is associated with a smaller M_{half} value than higher latitudes. In the PC case, it is found that M_{half} decreases with elevation, so that in general lower M_{half} values are obtained. The elevation dependence is less pronounced in the case of the NPC air mass, whereas the latitude dependence is slightly higher. The latter finding could be expected, since the pressure correction reduces air mass, and hence also the latitude-dependent spread. At more than 3100 m, Sonnblick stands out for the NPC air mass case with a M_{half} value close to 1.9. This is mainly due to latitude (47.05°N). In the PC case, this particular site is much closer to 1.5 since M_{half} is now 1.3. This suggests that the deviations caused by high elevation and high latitude partly compensate each other. For the second highest site, Izaña (2373 m), M_{half} is close to 1.5 in the NPC case,

and ≈1.1 in the PC case, i.e., at the opposite extreme. This also shows that there is strong variability among sites, which cannot be explained by elevation or latitude alone. Typically, commercial PV plants are located below 3000 m due to the unavailability of higher sites, low population density, or other reasons. Therefore, the Sonnblick results are considered marginal, and removed from further analysis.

As stated before, the PC results show a noticeable elevation dependence. Moreover, M_{half} is then always below 1.5. This indicates that the selection of M_{pc} = 1.5 would not be ideal to construct GTI reference spectra, as was also stated early on (Gonzalez and Ross, 1980; Ross, 1980; Ross and Gonzalez, 1980). Using an NPC air mass of 1.5 is not ideal either. Nevertheless, a rather symmetrical spread around M_{npc} = 1.5 and a lower elevation dependence are found. Furthermore, use of the NPC air mass of 1.5 results in the same zenith angle for sea level and any elevation, which is advantageous for application of the spectra. Therefore, an NPC air mass of 1.5 is used for high-elevation subordinate GTI reference spectra in what follows. This result underlines that, in the case of GTI, the appropriate PC air mass is lower for sites with higher elevation.

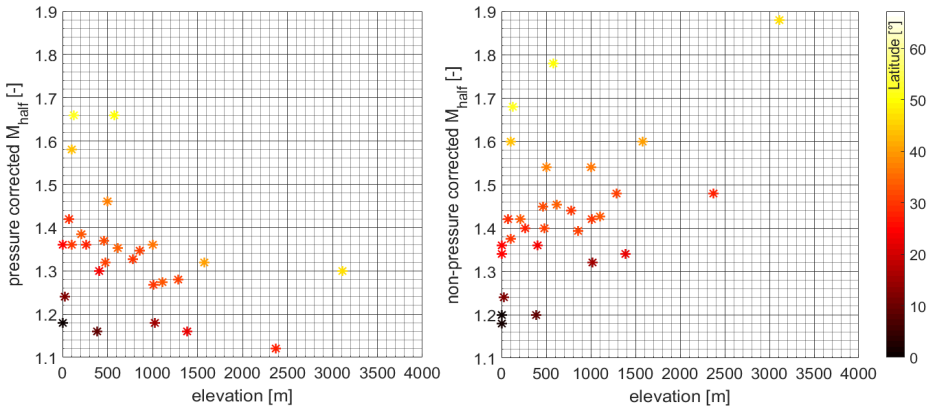

Fig. 6: M_{half} found for 29 sites for latitude-tilt GTI as a function of elevation and latitude (color bar). In the left plot two points are overlapping at elevation close to 0 m and M_{half} =1.18. This is also the case at elevation close to 0 and M_{half} =1.36.

Similar calculations are performed for DNI. Figure 7 presents the cumulative relative fraction of annual H_{b} as a function of air mass for sites below 750 m elevation. The differences between the plots for both air mass definitions are small, due to the low elevation of the sites. For the high-elevation sites in Fig. 8, the differences resulting from using pressure corrected or NPC air mass are clearly visible, due to the low atmospheric pressure at high elevation. The M_{half} values for DNI are shown in Fig. 9.

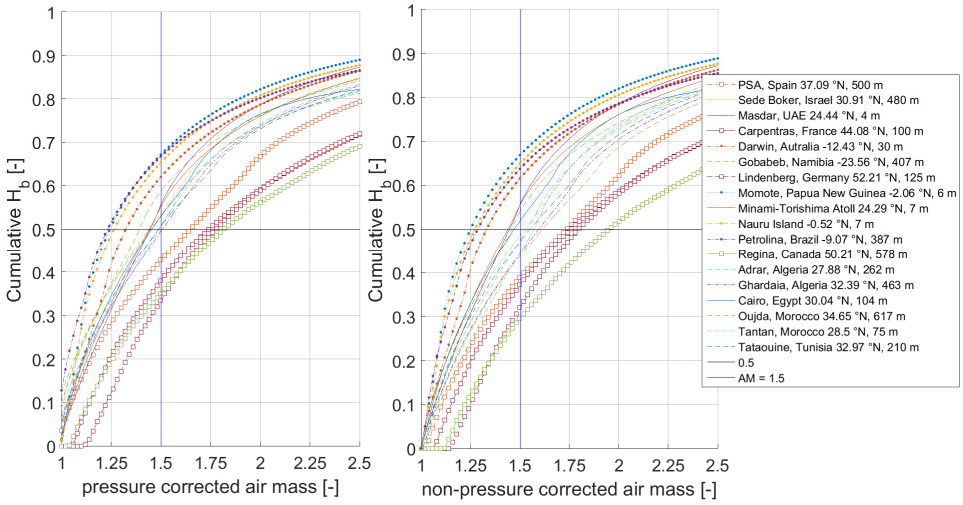

Fig. 7: Cumulative H_b over the air mass for sites below 750 m above mean sea level. Left: with pressure correction, right: without pressure correction. Sites less than 16° from the equator are marked with dots, sites with 37° or more by squares.

In addition to the sites discussed above for GTI, other sites analyzed by Emery et al. (2002) are presented. The latitude dependence is found similar to the case of GTI, albeit even more pronounced. Again, it is clear that the selection of a specific air mass value is not easy, or independent from the pressure-correction issue. Moreover, the highest sites (Sonnblick and Izaña) behave similarly for DNI and GTI. For the NPC air mass, Sonnblick has an M_{half} of 2.25, whereas M_{half} is only 1.52 for the PC case. In both cases, the 1.5 value is approximately midway between what is obtained for sites at high latitudes and sites near the equator, which supports the choice of

that value in the IEC/G173 standard spectrum. However, the elevation dependence of the PC cases is less pronounced for DNI than for GTI. The reverse is true in the NPC cases. The PC results also exhibit a smaller spread of M_{half} than those pertaining to the NPC air mass. This suggests a weak advantage of using the PC air mass definition for DNI. Hence, for DNI, these results are in relative agreement with previous studies (Emery et al., 2002; Gonzalez and Ross, 1980). Consequently, the application of a pressure-corrected air mass of 1.5 is selected here to evaluate the impact of using DNI spectra in spectral mismatch studies. Still, it is stressed that the approach described above and the resulting selection are not entirely satisfying in the case of DNI. Selection of a PC air mass of 1.5 means that higher zenith angles are representative at higher sites, a surprising result possibly explained in terms of Rayleigh transmittance as a function of site elevation. When the sun is at the zenith, the Rayleigh transmittances at 0-m and 1.5-km elevation are nearly identical. For a zenith angle of 80° the Rayleigh transmittance is noticeably lower at sea level due to the exponential behavior of transmittance (0.72 at sea level compared to 0.76 at 1.5 km for a Rayleigh OD of 0.05). Therefore, it could be true that lower air masses contribute more to H_b at higher elevations which means that greater zenith angles are more appropriate at higher elevations. However, both AOD and PW actually decrease with elevation in most cases. A typical scale height for them is 2.1 km, with large spatio-temporal variability, whereas that scale height is fixed at 8.43 km for both Rayleigh scattering and pressure. Therefore, the NPC air mass of 1.5 should also be considered for the DNI spectra. Since it is found problematic and potentially misleading to define subordinate DNI spectra (Jessen et al., 2018), the selection of the correct air mass is of low relevance in that case.

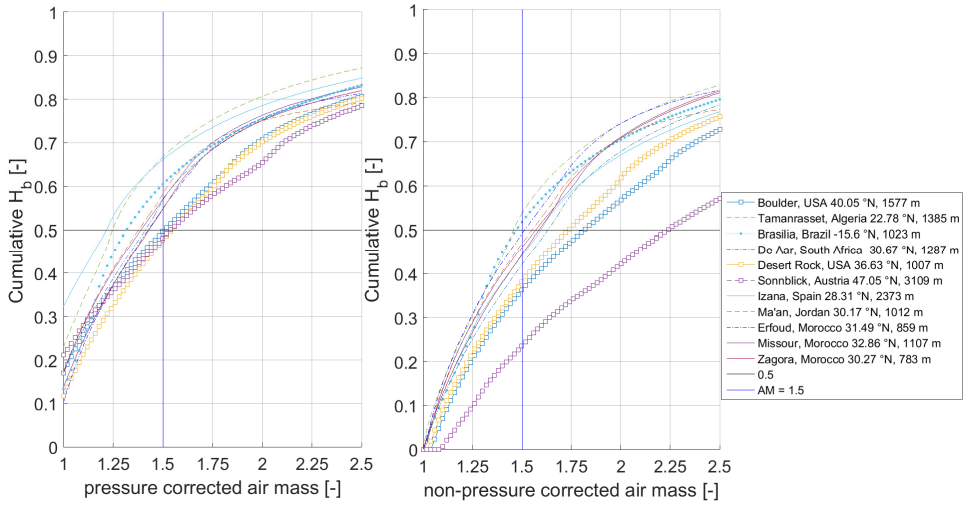

Fig. 8: Cumulative DNI over the air mass for sites at elevations above 750 m above mean sea level. Left: with pressure correction, right: without pressure correction. Sites less than 16° from the equator are marked with dots, sites with 37° or more by squares.

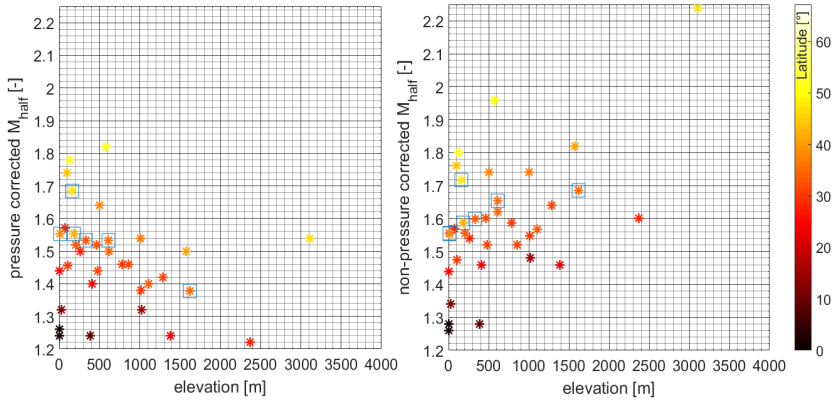

Fig. 9: M_{half} found for 36 sites for DNI as a function of the elevation and the latitude (color bar). Open blue squares mark additional sites from (Emery et al., 2002) (Albuquerque: 35.0853°N, 1619 m; Daggett: 34.8640°N, 610 m; Phoenix: 33.4484°N, 331 m; Tampa: 27.9506°N, 15 m; Sacramento: 38.5816°N, 9 m; Buffalo: 42.8864°N, 183 m; Seattle: 47.6062°N, 158 m).

3.2 Evaluation of air mass selection in terms of spectral mismatches

In order to test the two selections of the PC air mass of 1.5 for DNI and the NPC air mass of 1.5 for GTI, the effect of test spectra on the spectral mismatch is evaluated with different air masses. Two of the five aforementioned sites above 1-km elevation (Tamanrasset and Boulder) are useful to test the air mass specification. For this evaluation, the spectral mismatch values obtained with seven different spectra are compared for each site

and component (DNI or GTI). The reference spectrum in each case is the average spectrum for the site and component (see section 2). The spectral mismatch is calculated for these spectra:

1. ASTM G173/IEC 60904-3
2. The test spectrum for the atmospheric conditions in Tab. 1 that best match the average atmospheric conditions at the site, but for PC air mass M_{pc}=1.5
3. The test spectrum for the atmospheric conditions in Tab. 1that best matches the average atmospheric conditions at the site for NPC air mass M_{npc}=1.5
4. An ad-hoc spectrum specially developed for the site's average AOD, PW, elevation, and the M_{half} value for PC air mass $M_{half,pc}$ that is found for this specific site
5. An ad-hoc spectrum specially developed for the site's average AOD, PW, elevation, and the M_{half} value for NPC air mass $M_{half,npc}$ that is found for this specific site
6. An ad-hoc spectrum specially developed for the site's average AOD, PW, elevation, and M_{pc} = 1.5
7. An ad-hoc spectrum specially developed for the site's average AOD, PW, elevation, and M_{npc} = 1.5.

Moreover, for GTI the tilt angle is adjusted to the site's latitude in cases 4 to 7 just described. In cases 2 to 3 the closest available tilt angle (in 5° steps from 0 to 90°) is selected. For DNI, additionally, the two Ångström exponents for wavelength intervals below and above 0.5 µm are site-adapted in cases 4–7. Table 2 provides the values of M_{half} with and without pressure correction for GTI and DNI.

Tab. 2: M_{half} derived for Tamanrasset and Boulder from Fig. 5 and 8 with and without pressure correction for DNI and GTI.

Site	Component	$M_{half,pc}$, corresponding M_{npc} and standard conditions	$M_{half,npc}$
Boulder	GTI	1.325, corresponding to M_{npc} = 1.6 for ClDryHi	1.6
	DNI	1.5, corresponding M_{npc} = 1.81 for ClDryHi	1.82
Tamanrasset	GTI	1.15, corresponding to M_{npc} = 1.38 for SemClDryHi	1.35
	DNI	1.245, corresponding to M_{npc} = 1.5 for SemClDryHi	1.455

Figure 10 shows the seven DNI spectral mismatches for four CPV cell types under the seven DNI spectra at Tamanrasset. The different spectra are shown on the Y-axis, and mismatches for different PV cell types are shown by the marker type. The markers are connected to each other to increase readability. When using the base case of G173/IEC, deviations up to 4% are found. SemClDryHi behaves even worse than G173 in that case, so that if no pressure correction is applied even higher mismatch values are found. These deviations are mainly caused by Tamanrasset's average Ångström exponent that deviates strongly from that of SemClDryHi. Adjusting all atmospheric inputs to the site's averages reduces the mismatches noticeably for M_{npc} = 1.5, as well as the site's $M_{half,npc}$ and $M_{half,pc}$ (since all three cases result in the same input air mass). The spectrum for these site averages and M_{pc} = 1.5 results in the lowest spectral mismatch. This is surprising because the M_{half} values indicate that M_{npc} = 1.5 is more appropriate. The low spectral mismatches in this case are apparently caused by a compensation of errors. The average site spectrum also contains cloud effects and variations of the atmospheric properties that cannot be considered accurately when dealing with just a single spectrum. The approach using M_{half} is also only an approximation, as mentioned above.

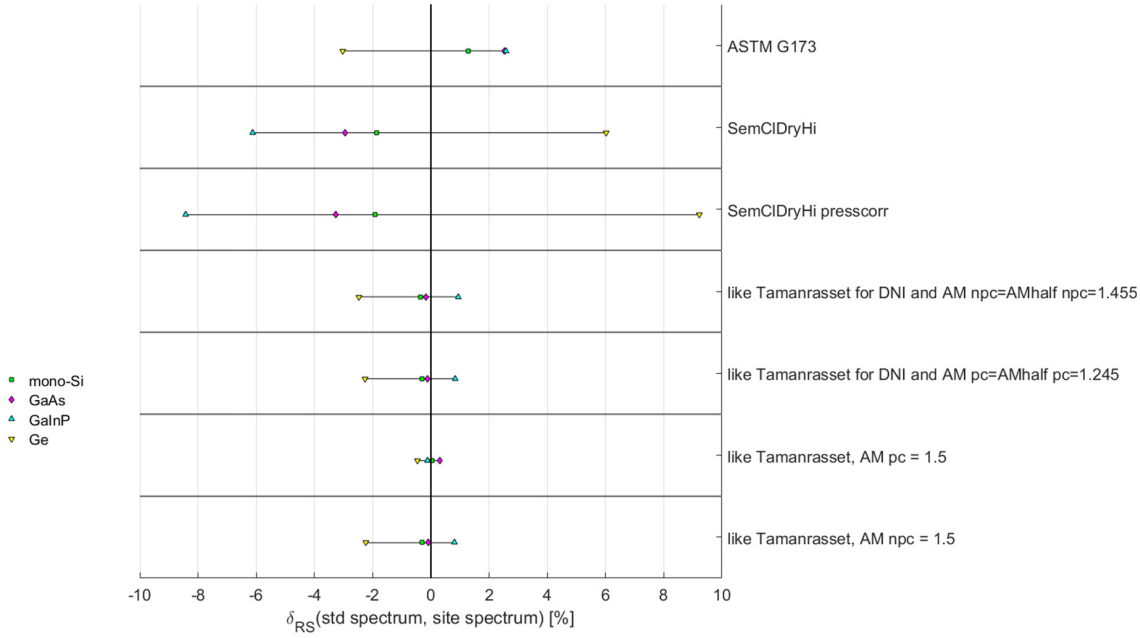

Fig. 10: ***Spectral mismatches for different spectra and CPV cell types for DNI at Tamanrasset.***

The results for Tamanrasset and DNI are summarized in Tab. 3 next to the other three cases, which are also shown in Figs. 11–13. The observations that do not correspond to expectations are marked in bold and underlined letters. The cases with more positive results than expected can be explained by the fact that several approximations and sources of error are included in the approach, and that different errors can compensate each other. The unexpected cases leading to worse results than G173 are marked with a minus sign. They are only found for DNI at Tamanrasset and have been explained above. Overall, it is found that the concept of using M_{half} is helpful, even though other air masses than those selected from M_{half} may perform better. This is interpreted as an effect of mutually compensating errors, too. The results confirm the expectation from section 3.1 that, for GTI, the NPC air mass of 1.5 can be used.

The results from Tab. 3 and Figs. 10 and 12 also show the aforementioned issues in the case of DNI. For Tamanrasset the Ångström exponent is found highly relevant. It can be concluded from this example that, due to the impact and variability of the Ångström exponent, a large number of subordinate DNI standard spectra would be needed to allow the selection of a subordinate spectrum that would be more representative than G173. Since this appears impractical, no subordinate standard spectrum is recommended here for DNI.

For DNI at Boulder, the actual Ångström exponent is similar to that characterizing all 7 test spectra. If site averages of the Ångström exponents, AOD and PW are used, the PC air mass of 1.5 delivers better results than the NPC value of 1.5, as expected. Even if the site averages for all significant inputs are used, greater deviations are found in comparison to GTI due to the high sensitivity of the DNI spectrum to air mass and atmospheric conditions, again as expected.

Tab. 3: Results of the evaluation of spectral mismatch based on air-mass selection. The + sign means improvement compared to G173/IEC, and the – sign means greater spectral errors than G173/IEC. Brackets refer to lower tendency than a sign without brackets, and various signs refer to higher differences. The * symbol means that a low spectral mismatch is found due to mutual compensation of errors. Cases with deviations from the expected behavior are underlined.

Spectrum	Tamanrasset DNI	Tamanrasset GTI	Boulder DNI	Boulder GTI
1. IEC/G173	-4 – 3 %	0.5% - 4.5 %	-7.5 % - 7 %	2 -5 %
2. test M_{pc}=1.5	**-**	+, for a-Si1 worse than G173	**(+)**	((+))
3. test M_{npc}=1.5	**-**	**++, ***	((+))	**++, ***
4. site's average parameters $M_{half,pc}$	+, same as 5 and 7	+(+), same as 5	((+)), same as 5 and 6	+(+), same as 5
5. site's average parameters $M_{half,npc}$	+, same as 4 and 7	+(+), same as 4	((+)), same as 4 and 6	+(+), same as 4
6. site's average parameters M_{pc} = 1.5	**++, ***	(+)	((+)), same as 4 and 5	(+)
7. site's average parameters M_{npc} = 1.5	+, same as 4 and 5	+ only for a-Si2 worse than case 6	(((+)))	**++**

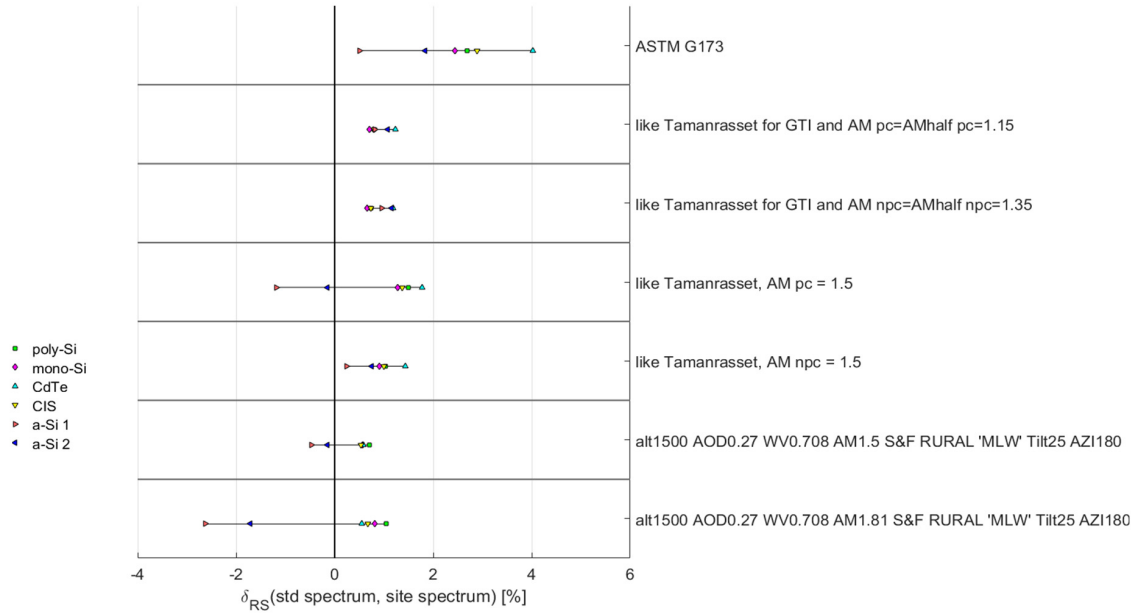

Fig. 11: ***Spectral mismatches for different spectra and PV cell types for GTI and Tamanrasset. The lower two spectra refer to SemClDryHi for the tilt angle 25° with and without pressure correction.***

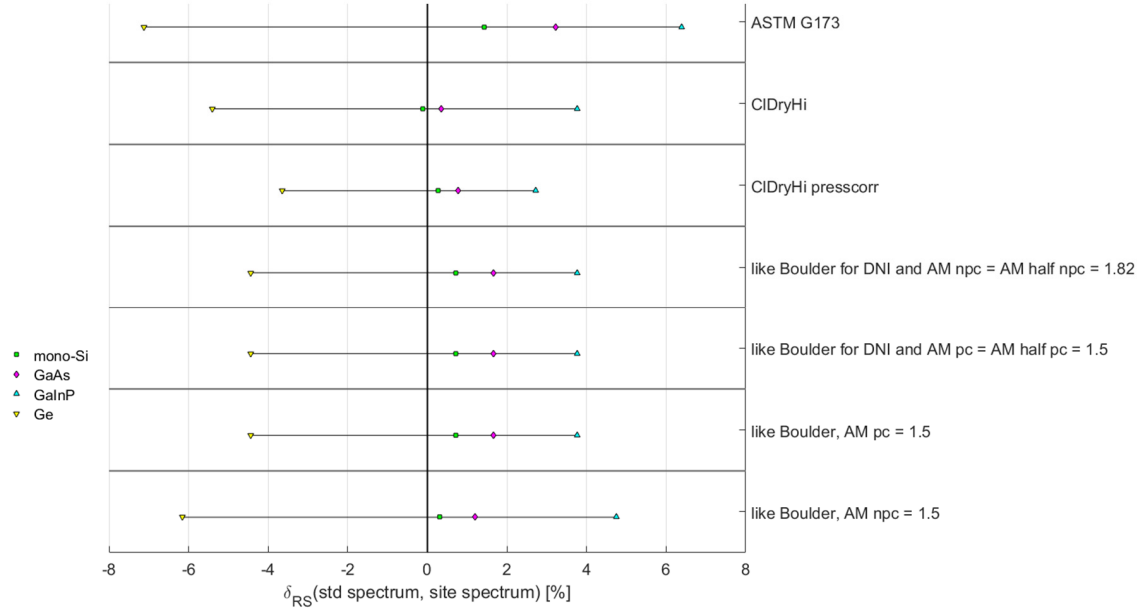

Fig. 12: ***Spectral mismatches for different spectra and CPV cell types for DNI and Boulder.***

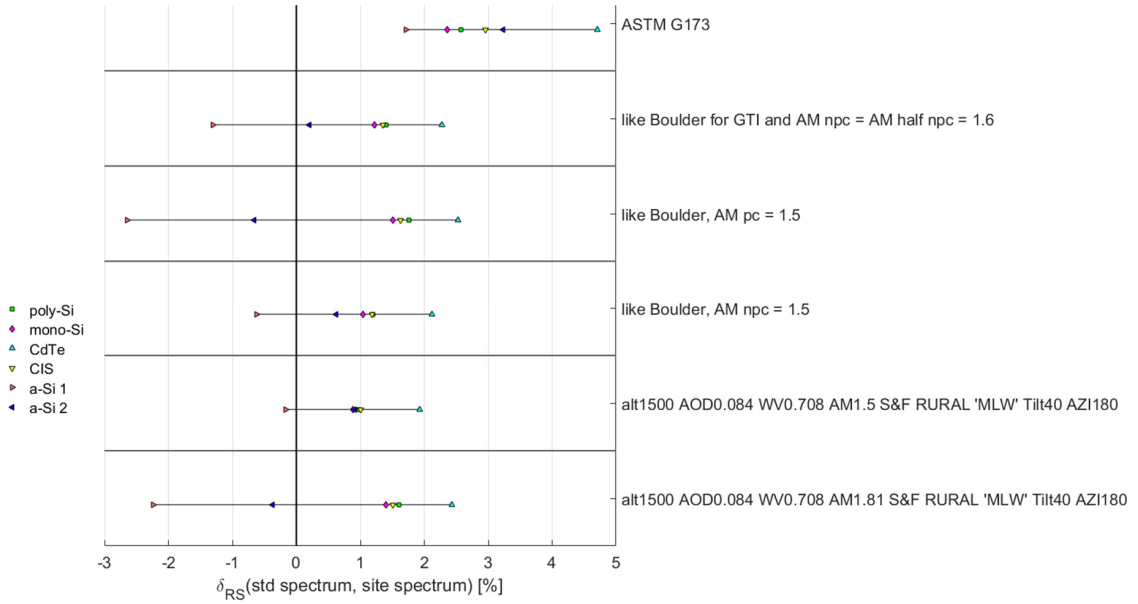

Fig. 13: ***Spectral mismatches for different spectra and PV cell types for GTI and Boulder. The lower two spectra refer to ClDryHi for the tilt angle 40° with and without pressure correction.***

4. Conclusion and outlook

The impact of different climatic conditions on the solar spectrum at the surface, and its consequences for solar energy system performance, reveals that the IEC/G173 standard spectra are far from representing the wide range of locally occurring conditions. Subordinate standard spectra are proposed here for solar energy applications utilizing GTI. They are meant to supplement the main standard spectra as defined in IEC/G173. These subordinate spectra represent atmospheric conditions and sun-receiver geometries that result in incident spectra departing significantly from the existing standard spectra. Some of the subordinate spectra correspond to site elevations of 1.5 km, since such higher-elevation sites are of interest in many solar energy applications. To apply the subordinate spectra, manufacturers could include PV module efficiencies for the different subordinate spectra in their data sheets. A potential customer could then identify the efficiency for the most appropriate subordinate spectra that is found using simple climate parameters, the site's elevation and the tilt angle.

The selection of the correct air mass to use in subordinate spectra is based on an analysis of the cumulative DNI and GTI for different air-mass ranges at 29 sites. A clear latitude dependence of the most appropriate air mass

for each site is found, so that using an air mass of 1.5 must be considered a crude approximation in any case. Overall, it is found that the pressure-corrected air mass value of 1.5 is more appropriate for DNI spectra, but not for GTI, thus confirming earlier studies. A non-pressure-corrected air mass of 1.5 is found more appropriate for GTI. Even though a pressure-corrected air mass is deemed preferable for DNI, the justification is weak. Physical explanations rather suggest that the pressure correction is actually not appropriate in that case. This is not an issue here, however, as we only recommend GTI subordinate spectra, but not DNI spectra. Indeed, it is found that there are no ideal subordinate spectra for DNI. Many subordinate DNI spectra for a large range of atmospheric conditions would be required to reduce the spectral mismatch compared to IEC/G173. It would thus be difficult to select the most appropriate spectrum, which is not practical. Hence, it is recommended not to include any subordinate DNI spectrum in the forthcoming ISO 9845 update.

The finding that a non-pressure corrected air mass of 1.5 is appropriate for GTI was confirmed by evaluating the spectral mismatch obtained for several PV cell types at the high-elevation sites of Boulder and Tamanrasset, using different test spectra. Hence, subordinate GTI spectra with the proposed atmospheric conditions, tilt angles, and non-pressure corrected air mass of 1.5, are recommended for inclusion in the update of ISO 9845, as an addition to the existing IEC or ASTM standard spectra. Comments on the proposed spectra are welcome and can be considered in the ISO and ASTM committees.

We thank the investigators and their support teams for the maintenance of the AERONET, enerMENA and BSRN stations used in this work. We thank the Actris and AERONET staff for their support with the operation, calibration and evaluation of PSA's and Masdar's sun photometer. This work was partly funded by the Helmholtz Association within the DESERGY Project. The financial support provided to the University of Antofagasta by the Chilean Economic Development Agency, CORFO, contract no. 17PTECES-75830 and the contract no.: 17BPE3-83761, and CONICYT/FONDAP/15110019 SERC-Chile is acknowledged.

5. References

Dirnberger, D., G. Blackburn, B. Müller, C. Reise, On the impact of solar spectral irradiance on the yield of different PV technologies, Solar Energy Materials and Solar Cells 132 (2015) 431–442.

Emery, K., Myers, D., and Kurtz, S., 2002. What is the appropriate reference spectrum for characterizing concentrator cells? 29th IEEE PV Specialists Conference, New Orleans, LA.

Fernández, E.F., F. Almonacid, J.A. Ruiz-Arias, A. Soria-Moya, Analysis of the spectral variations on the performance of high concentrator photovoltaic modules operating under different real climate conditions, Solar Energy Materials and Solar Cells. 127 (2014) 179–187. doi:10.1016/j.solmat.2014.04.026.

Gueymard, C., 2001. Parameterized transmittance model for direct beam and circumsolar spectral irradiance. Solar Energy 71 (5):325-346.

Gueymard, C.A., Myers, D., Emery, K., 2002. Proposed Reference Irradiance Spectra for Solar Energy Systems Testing. Solar Energy 73, 443-467.

Gueymard, C.A., 2005. SMARTS Code version 2.9.5 User's Manual. Solar Consulting Services.

Gueymard, C., 2012. Solar Radiation, Introduction, in: Meyers, R.A. (Ed.) Encyclopedia of Sustainability Science and Technology, Springer, pp. 608-633.

Gonzalez, C.C., Ross R.G., 1980. Performance Measurement Reference Conditions for Terrestrial Photovoltaics, Proc. Conf. American Section of the International Solar Energy Soc., Phoenix, Arizona, 1401–1405.

IEC 60904-3:2016 Photovoltaic devices - Part 3: Measurement principles for terrestrial photovoltaic (PV) solar devices with reference spectral irradiance data. Standard, Geneva, Switzerland.

Jessen, Wilko, Stefan Wilbert, Christian A. Gueymard, Jesús Polo, Zeqiang Bian, Anton Driesse, Aron Habte, Aitor Marzo, Peter R. Armstrong, Frank Vignola, and Lourdes Ramírez. 2018. "Proposal and evaluation of subordinate standard solar irradiance spectra for applications in solar energy systems." Solar Energy. https://doi.org/10.1016/j.solener.2018.03.043.

Kalapatapu, R. Chiesa, M., Armstrong, P., Wilbert, S., 2012. Measurement of DNI Angular Distribution with a Sunshape Profiling Irradiometer. SolarPACES Conf., Marrakesh, Morocco.

König-Langlo, G., Sieger, R., Schmithüsen, H., Bücker, A., Richter, F., Dutton, E.G. 2013. The Baseline Surface Radiation Network and its World Radiation Monitoring Centre at the Alfred Wegener Institute. GCOS - 174, WCRP Report 24/2013.

Kopp, G., and J. L. Lean, 2011. A new, lower value of total solar irradiance: Evidence and climate significance, Geophys. Res. Lett., 38, L01706, doi:10.1029/2010GL045777.

Nann, S. and Riordan, C., 1991. Solar spectral irradiance under clear and cloudy skies: Measurements and a

semiempirical model. J. Appl. Meteorol. 30, 447–462.

Nofuentes, G., Gueymard, C.A., Aguilera, J., Pérez-Godoy, M.D., Charte, F., 2017. Is the average photon energy a unique characteristic of the spectral distribution of global irradiance? Solar Energy 149, 32–43.

Polo, J., M. Alonso-Abella, J.A. Ruiz-Arias, J.L. Balenzategui, Worldwide analysis of spectral factors for seven photovoltaic technologies, Solar Energy. 142 (2017) 194–203. doi:10.1016/j.solener.2016.12.024.

Pozo-Vázquez, D., S. Wilbert, C. Gueymard, L. Alados-Arboledas, F. J. Santos-Alamillos, and M.J. Granados-Muñoz. 2011. Interannual Variability of Long Time Series of DNI and GHI at PSA, Spain. Paper read at SolarPACES Conference, at Granada, Spain.

Ross, C.C., 1980. Terrestrial Photovoltaic Performance Reference Conditions. Proc. Photovoltaic Solar Energy Conf., Cannes, France, 731–735.

Ross, R.G. and Gonzalez, C.C., 1980. Reference conditions for reporting terrestrial photovoltaic performance. Proc. AS/ISES Annual Conf., 1091–1097.

Schüler, D., Wilbert S., Geuder N., Affolter R., Wolfertstetter F., Prahl C., Röger M., Schroedter-Homscheidt M., Abdellatif G., Allah Guizani A., Balghouthi M., Khalil A., Mezrhab A., Al-Salaymeh A., Yassaa N., Chellali F., Draou D., Blanc P., Dubranna J., Sabry O. M. K., 2016. The enerMENA meteorological network – Solar radiation measurements in the MENA region. AIP Conference Proceedings no. 1734 (1):150008.

Wilbert, S., B. Reinhardt, J. DeVore, M. Röger, R. Pitz-Paal, C. Gueymard, and R. Buras, 2013. Measurement of solar radiance profiles with the Sun and Aureole Measurement system. J. Solar Energy Engineering 135 (4):041002-041002. doi: 10.1115/1.4024244.

Skartveit, A., Olseth, J.A., 1986. Modelling slope irradiance at high latitudes. Solar Energy 36, 333–344.

Winter, S., Friedrich, D., and Sperling, A., 2009. Effects of the new standard IEC 60904 3:2008 on the calibration results of common solar cell types. 24th European Photovoltaic Solar Energy Conf., Hamburg, Germany.

WMO, 2014. Guide to Meteorological Instruments and Methods of Observation. WMO-No. 8, 2014 Update.